FIELD AND ENERGY-DENSITY PROFILES IN LAYERED SUPERCONDUCTOR-DIELECTRIC STRUCTURES

J. M. Pond
Microwave Technology Branch
Naval Research Laboratory, Washington, DC 20375-5000

and

P. Weaver
Department of Electrical Engineering
University of Hawaii, Honolulu, HI 96822

Abstract — The electromagnetic field profiles and energy densities for some layered superconductor-dielectric structures are calculated. Of particular interest is the situation when the superconducting film is thinner than the superconducting penetration depth. In these cases the primary energy storage mechanism in the superconductor is the inertial energy stored in the superconducting current rather than the magnetic field. An understanding of the arrangement of electromagnetic fields in layered superconductor-dielectric structures will aid in the development of circuits and devices which utilize these properties.

I. INTRODUCTION

The decay length of a magnetic field into a superconductor is called the penetration depth, λ [1,2], and, hence, is analogous to the skin depth in normal metals. Since a magnetic field exists in the surface of a superconductor, magnetic energy is stored in the superconductor and can be represented as a magnetic inductance, L_m. Another energy storage mechanism which exists in the superconductor is the kinetic energy of the superconducting current. This energy term can be accounted for by a kinetic inductance, L_k. For a very thick superconductor, the inductance due to both of these energy storage mechanisms is equal if the London model is used [3]. For very thin super-conductors, L_k can be orders of magnitude larger than L_m [4].

A superconductor allows guided wave geometries to be considered where significant percentages of the fields are contained within the superconductor rather than in a dielectric region. In contrast, the use of a normal conductor in a similar geometry would result in large losses. A number of microwave components have been proposed and built which rely on taking advantage of this unique property of thin superconductors [4-7]. Since many of these concepts utilize the large L_k effect of thin superconducting layers and one or more dielectric layers, a detailed examination of several illustrative examples can impart a greater understanding of the arrangement of electromagnetic fields in layered superconductor-dielectric structures. This paper examines the behavior of the fields and energy densities in layered dielectric-superconductor structures. The equations governing electromagnetic fields and energy in superconductors are reviewed. The numerical implementation of the solution for some illustrative examples is then presented followed by a discussion of a number of field and energy-density plots.

II. FOUNDATION

Assuming Londons' equations and the two-fluid model are applicable to the superconductors, the current is given by

$$\vec{J} = \vec{J}_s + \vec{J}_n = \left(\omega \mu_0 \lambda^2\right)^{-1} \vec{E} + \sigma_n \vec{E} \tag{1}$$

where the subscripts s and n denote the superconducting and normal currents, respectively. From Londons' equations:

$$\nabla x \vec{J}_s = -\lambda^{-2} \vec{H} \quad \text{and} \quad \mu_0 \partial \vec{J}_s / \partial t = \lambda^{-2} \vec{E} \tag{2}$$

The relationship between J_s and E is consistent with the concept of describing the stored kinetic energy as an inductance. J_n, due to the carriers in the normal state, follows from Ohm's law.

Assuming an $e^{j\omega t}$ time dependence the integral form of the time average power-energy conservation theorem is:

$$\oint_s \mu_0^{-1} \left(\vec{E} x \vec{B^*}\right) \cdot \hat{n} dS - j\omega \int_v \left(\varepsilon_0 \vec{E} \cdot \vec{E^*} - \mu_0^{-1} \vec{B} \cdot \vec{B^*}\right) dV + \int_v \left(\vec{E} \cdot \vec{J^*}\right) dV = 0 \tag{4}$$

since, in a superconductor $\mu = \mu_0$ and $\varepsilon = \varepsilon_0$. The third integral represents energy dissipated (normal current) and energy stored (superconducting current). Hence, Eqn. 4 can be rewritten as:

$$\frac{1}{2} \oint_s \left(\vec{E} x \vec{B^*}\right) \cdot \hat{n} dS - \frac{j\omega}{2} \int_v \sigma_n \vec{E} \cdot \vec{E^*} dV - \frac{j\omega}{2} \int_v \left\{\left[\varepsilon_0 - \left(\omega^2 \mu_0 \lambda^2\right)^{-1}\right] \vec{E} \cdot \vec{E^*} - \mu_0 \vec{B} \cdot \vec{B^*}\right\} dV = 0 \tag{5}$$

The real part of (5) says that the time average real power transferred across S is equal to the time average power transferred to the normal electrons in V. The imaginary part of (5) says that the time average imaginary power transferred across S is equal to the difference between time average electric energy and sum of the time average kinetic and magnetic energies stored in V. The kinetic energy of the superconducting current is proportional to the square of the electric field strength but has the same sign as the magnetic energy, consistent with the terminology of L_k.

III. FORMULATION

Two guided-wave structures are studied. Fig. 1 shows a structure consisting of two thin superconducting films separated by a dielectric. Fig. 2 shows three thin superconducting films separated by two thin dielectric layers. Electromagnetic field solutions to these structures are considered which correspond to the dominant guided-wave modes. Thus, only the lowest order TM modes, propagating along the z axis, exist and hence $H_x = H_z = E_y = 0$. The field components in region n are given by

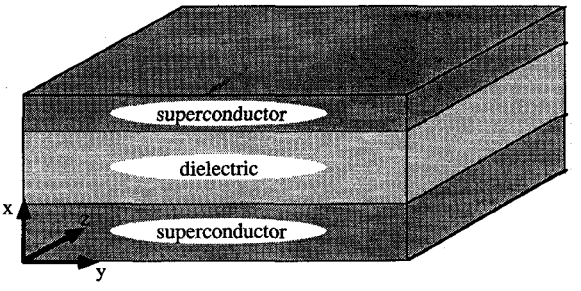

Figure 1. General geometry for a structure composed of two superconducting layers separated by a dielectric layer.

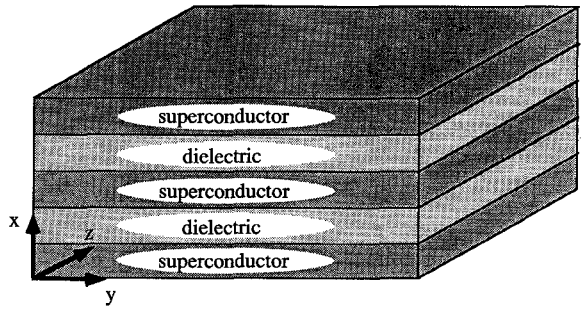

Figure 2. General geometry for a structure composed of three superconducting layers each separated by a dielectric layer.

$$\vec{H} = \hat{y}\left\{C_n^- e^{-\gamma_{x_n} x} + C_n^+ e^{\gamma_{x_n} x}\right\} e^{j(\omega t - k_{z_n} z)} \qquad (6)$$

and Maxwell's equations. Hence, E_x and E_z are the only other non-zero field components. From Eqn. 5 and the geometry shown in Figs. 1 and 2, it follows that the superconducting current arises primarily from E_z. Approximate closed-form dispersion equations have been previously derived for both structures [3, 7]. The second structure is a coupled line problem with two dominant modes corresponding to a generalized even mode (c-mode) and a generalized odd mode (π-mode). The coupling between the parallel plate regions is provided by the penetration of the fields through the common superconductor.

The approximate closed-form dispersion equations for these structures, although yielding accurate information about the phase velocity, v_p, and attenuation, are not sufficiently accurate to reconstruct the field and energy-density profiles, but were used to provide an initial guess. Instead, a numerical implementation of the transverse resonance method was used to accurately determine the roots corresponding to the dominant guided-wave modes.

III. RESULTS

Field profiles are shown in Fig. 3 for the structure of Fig. 1. It is assumed that the center dielectric region has a relative permittivity of 10.0, the superconductors have a penetration depth of 300 nm at T = 0 (λ_0 = 300 nm), and the operating temperature is $0.33T_C$. These values were used in all calculations unless otherwise noted. The amplitude of E_x was arbitrarily set to unity at the center of the dielectric region. Fig. 3 shows the behavior of the field components for several values of superconductor and dielectric layer thickness which, for presentation convenience, were assumed to be all the same thickness. Fig. 3a, 3b, and 3c show the field profiles when the layer thickness are all equal to 30 nm ($0.1\lambda_0$), 300 nm ($1.0\lambda_0$), and 3000 nm ($10.0\lambda_0$), respectively. Fig. 4a, 4b, and 4c, show the profiles for the electric, magnetic and kinetic energy densities for the same three cases. As the superconducting layer thickness becomes small compared to λ, the stored energy becomes dominated by the kinetic energy of the superconducting current which corresponds directly with the behavior of E_z. When the superconductor is thick compared to λ, the kinetic energy and magnetic energy in the superconductor are virtually identical.

Field profiles, for the structure of Fig. 2, are shown in Figs. 5, and 6. It was assumed that both dielectrics were 100 nm thick and that the outer superconductors were 20 nm thick. Figs. 5a, 5b, and 5c show the behavior of E_x, E_z, and H_y, respectively, when the center superconductor is 20 nm thick. Figs. 6a, 6b, and 6c show the behavior of E_x, E_z, and H_y, respectively, when the center superconductor is 100 nm thick. The v_p of the two dominant modes of this structure have been

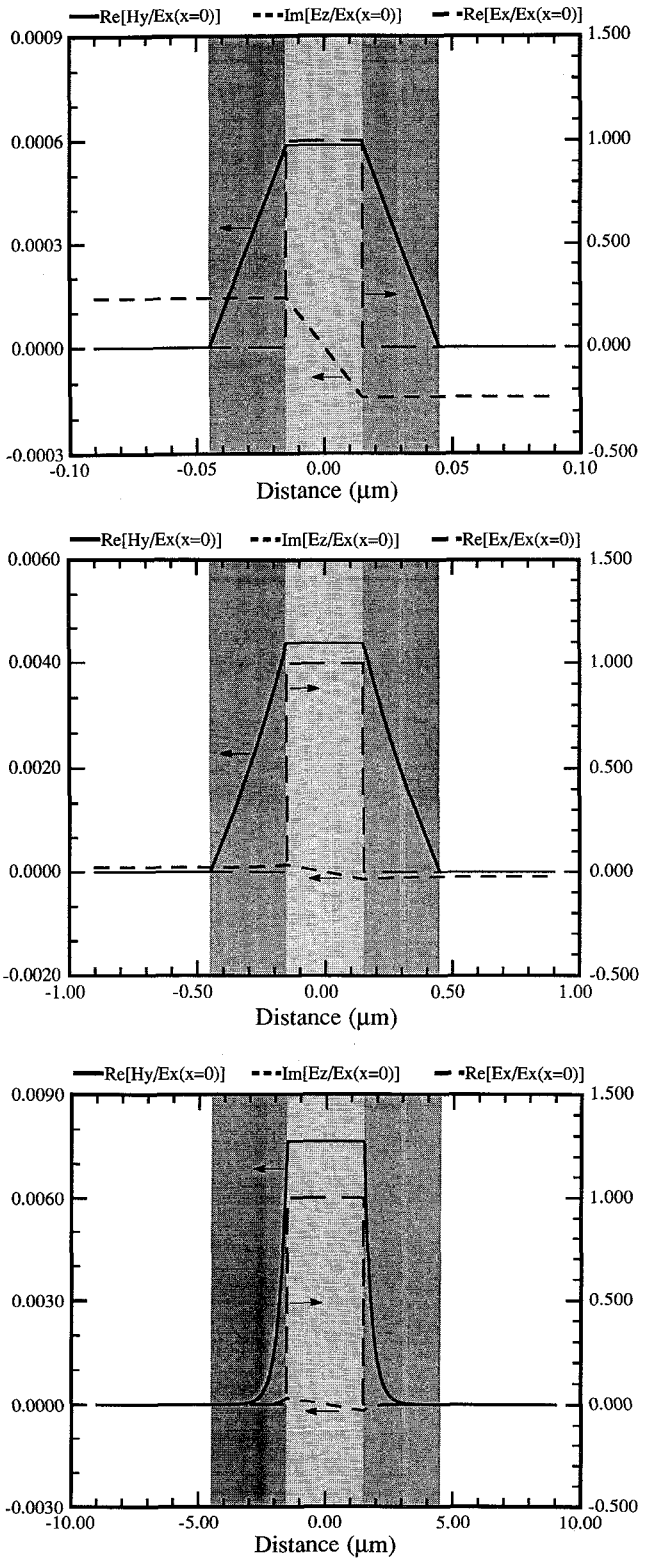

Figure 3. Field profiles for the structure of Fig. 1 when each layer is: a) 30nm thick ($0.1\lambda_0$), b) 300nm thick ($1.0\lambda_0$), c) 3000nm thick ($10.0\lambda_0$). For clarity, the superconducting regions are shaded dark gray while the dielectric regions are shaded light gray. The amplitude of E_x is set to unity at the center of the dielectric.

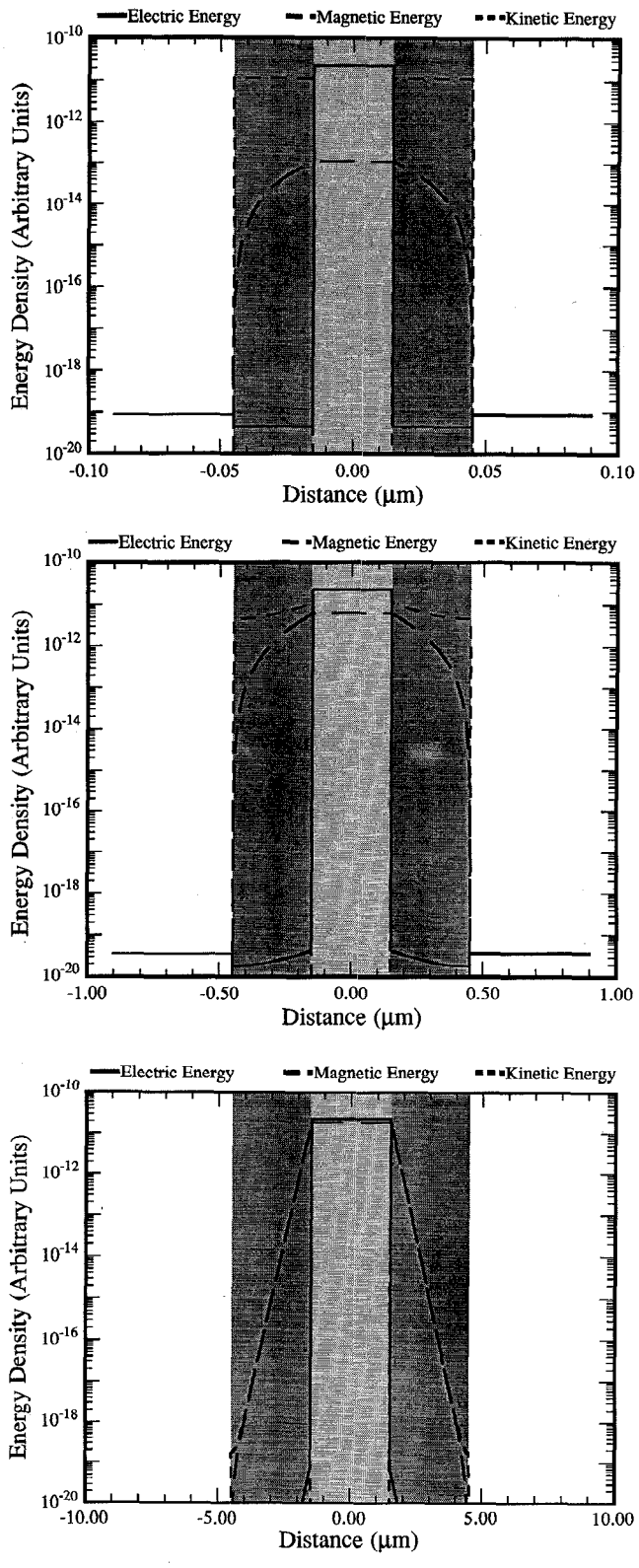

Figure 4. Energy-density profiles for the structure of Fig. 1 when each layer is: a) 30nm thick ($0.1\lambda_0$), b) 300nm thick ($1.0\lambda_0$), c) 3000nm thick ($10.0\lambda_0$). The superconducting regions are shaded dark gray while the dielectric regions are shaded light gray. The amplitude of E_x is set to unity at the center of the dielectric.

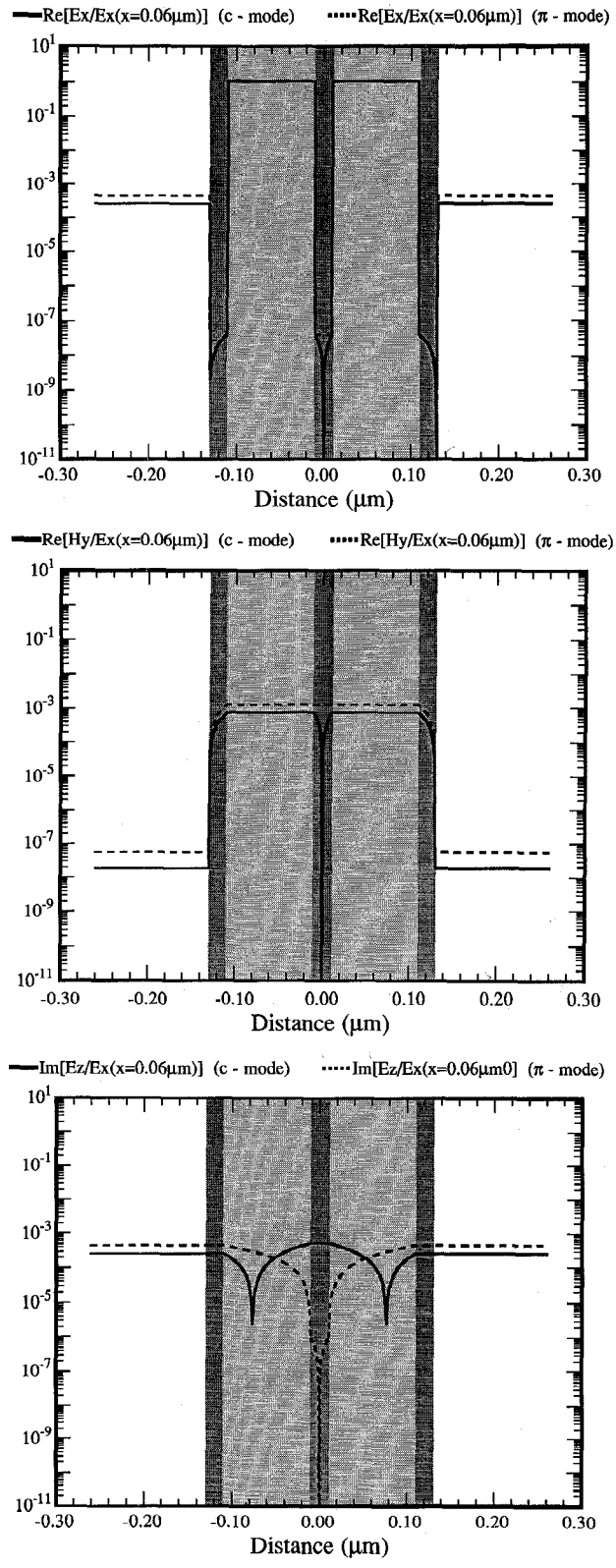

Figure 5. Field profiles for the structure of Fig. 2. The dielectric regions (light gray) are 100 nm thick, the outer superconductors (dark gray) are 20 nm thick and the center superconductor (dark gray) is 20nm thick. The normal electric, tangential electric, and tangential magnetic fields are shown in a), b), and c), respectively.

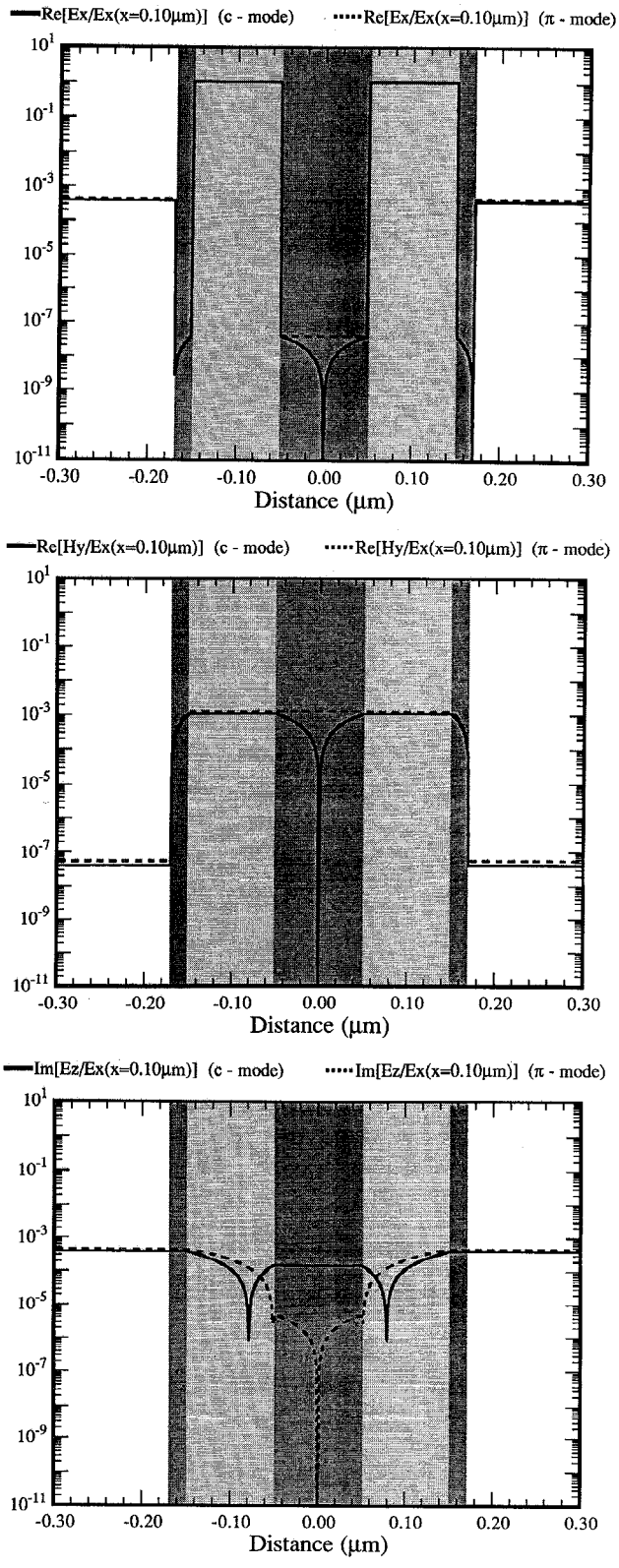

Figure 6. Field profiles for the structure of Fig. 2. The dielectric regions (light gray) are 100 nm thick, the outer superconductors (dark gray) are 20 nm thick and the center superconductor (dark gray) is 100nm thick. The normal electric, tangential electric, and tangential magnetic fields are shown in a), b), and c), respectively.

shown to behave quite differently as a function of the thickness of the center superconductor [7]. The v_p of the generalized even mode (c-mode) becomes much smaller as the center superconductor gets thinner. In contrast, the v_p of the generalized odd mode (π-mode) remains virtually constant. This behavior follows directly from an examination of the plots of E_z in Figs. 5b and 6b. For the c-mode, E_z in the center superconductor becomes larger as the center superconductor becomes thinner. The increasing concentration of E_z in the center superconductor as the center superconductor gets thinner means an increasing storage of kinetic energy in the superconducting current. This implies an increasing inductance per unit length and hence a decrease in v_p. In contrast, it is seen that for the π-mode E_z in the center superconductor actually goes through zero and, hence, there is little storage of kinetic energy in the superconducting current in this layer for this mode. Thus the inductance per unit length is virtually independent of the center layer thickness and, hence, there is little effect on v_p.

IV. Conclusions

Field and energy-density profiles have been calculated for layered superconductor-dielectric structures. The transverse resonance method was implemented numerically to determine the complex roots of the guided modes. Profiles of the fields and energy densities were obtained to yield a better insight into the design of novel circuit components which utilize kinetic inductance. Unlike with a normal metal, this mechanism can be the dominant mechanism for energy storage. Since new microwave components are possible [4-7], an appreciation of potential limitations is needed. In particular, the storage of large amounts of energy in thin superconductors implies very large superconducting current densities. Field and energy-density profiles can be useful in assuring that the superconducting current density will not exceed the critical current density of the superconductor.

Acknowledgment

The authors would like to thank Mr. M. Reuss, and Dr. M. Nisenoff for helpful discussions. This work was supported, in part, by the Office of Naval Research.

References

[1] T. VanDuzer and C. W. Turner, *Principles of Superconductive Devices and Circuits*. New York: Elsevier, 1981.

[2] F. London, *Superfluids, vol. I: Macroscopic Theory of Superconductivity*, New York: Dover Publications, 1961.

[3] J. C. Swihart, "Field solution for a thin-film superconducting strip transmission line," *J. Appl. Phys.*, vol. 32, no. 3, pp. 461-469, March. 1961.

[4] J M. Pond, J .H. Claassen, and W L. Carter, "Measurements and modeling of kinetic inductance microstrip delay lines," *IEEE Trans. Microwave Theory Tech.*, vol. MTT-35, no.12, pp. 1256-1262, December. 1987.

[5] C. S. Owen and D. J. Scalapino, "Inductive coupling of Josephson junctions to external circuits," *J. Appl. Phys.*, vol. 41, no. 5, pp. 2047-2056, April 1970.

[6] K. Yoshida, T. Nagatsuma, S. Kumataka, and K. Enpuku, "Millimeterwave emission from Josephson oscillator through thin film junction electrode," *IEEE Trans. Magn.*, vol. MAG-23, no. 2, pp. 1283-1286, March 1987.

[7] J. M. Pond, P. Weaver, and I. Kaufman, "Propagation characteristics of inductively-coupled superconducting microstrip," 1989 IEEE MTT-S International Microwave Symp. Dig., vol. 1, pp. 451-454, June, 1989.